INTERNATIONAL SCIENTIFIC JOURNAL
GEOGRAPHICA PANNONICA
Volume 28, Issue 3, 182–204 (September 2024)
Journal homepage: http://www.dgt.uns.ac.rs/en/homepage/pannonica/

Assessment of the Spatial Configuration Pattern in Tiruchirappalli City for Energy Studies through Generative Urban Prototype Models: A Case for Warm and Humid Climate

G. R. Madhavan[A*], Dr D. Kannamma[A]

[A] *Department of Architecture, National Institute of Technology, Tiruchirappalli, Tamil Nadu, India*

KEYWORDS

local climatic zones
image classification
urban morphology
cooling load consumption
machine learning
climate change

ABSTRACT

Developing countries with complex urban spatial configurations strive to control urbanization and its impact on energy consumption. The current study has used Tiruchirappalli city in India as a study area to demonstrate the impact on cooling energy consumption by complex urban spatial configurations. To comprehend the complexity, sixty-five urban prototypes were generated through permutation and combination using local climatic zones scheme. The image-based binary classification model was used to categorize the morphologies in the city. The study aims to investigate the cooling energy consumption of a heterogeneous urban spatial configuration through prototype models. The urban prototypes were grouped using the unsupervised machine learning approach. The validation for the prototypes was conducted through the RMSE method, and the errors lie between 0.45 and 0.68. The results indicated that increasing the green cover ratio on the combination of high and mid-rise spatial configurations is ineffective in reducing the cooling energy. In contrast, the combination of low-rise and mid-rise spatial configurations consumed less energy for air-conditioning when the green cover ratio was increased. The results conclude that the combination of high-rise with open low-rise spatial configuration is unsuitable for warm and humid climate. The high frequency of the cooling energy was between 120Gjs to 250Gjs which explains that the complexity of the spatial configuration in the city helps to reduce the energy utilized for air conditioning. This research aids planners and energy policymakers in the decision-making process of city spatial planning.

Introduction

In the last few decades, the world has undergone high urbanization as a result of population growth and the rise of cities (Sun et al., 2020). The life expectancy of the citizens living in highly populated cities has been reduced drastically. Urban population encounters major difficulties pertaining to thermal conditions and the energy sources necessary for sustaining a comfortable indoor environment (Ellena et al., 2020). Since the urban population has increased over the past few decades, temperatures in cities have been rising rapidly (Rajagopal et al.,

* Corresponding author: G. R. Madhavan, e-mail: madhavangr3@gmail.com

doi: 10.5937/gp28-50781

Received: May 01, 2024| Revised: August 31, 2024| Accepted: September 06, 2024

2023). Several cities have seen increased temperatures due to urbanization and climate change (Hood, 2005). In the 21st century, high-temperature occurrences are expected to become more frequent and longer (Dosio et al., 2018; Perkins-Kirkpatrick & Lewis, 2020). A study conducted by Heaviside et al. (2017) demonstrates that urban inhabitants have greater health risks than rural populations, particularly during high temperatures. The occurrence of heat waves further intensifies this risk. Numerous research has been conducted on the urban environment and microclimate to reduce the high-temperature occurrence in the coming years (Abougendia, 2023). The spatial arrangements of the built environment create thermal anomalies between cities and rural landscapes, which is deduced by the urban heat island intensity (Abougendia, 2023; Taha, 1997). UHI phenomenon is explained by different cooling rates between urban and rural areas (Klysik & Fortuniak, 1999). UHI intensity has been studied and reported by various authors (Arnfield, 2003; Masson et al., 2020; Oke, 2004; Stewart, 2011), and the temperature differences recorded in the research were based on urban morphology, land use pattern and climate (Nastran et al., 2019; Yue et al., 2019). Previous research on UHI addressed thermal anomalies up to 10°C (Alcoforado et al., 2014; Warren et al., 2016). The UHI intensity causes heat-related health risks in the residents of cities, along with increased cooling load consumption (Barrao et al., 2022). In the wave of urbanization, reducing cooling load consumption in the cities is the top priority (Vallati et al., 2015). Urban energy performance has become a worldwide environmental conversation in every decennial since global urbanization is expected to reach about 70% by 2050 (United Nations, 2019). The urban morphology significantly increases energy usage (Katal et al., 2022). A study by X. Li et al. (2019) shows that the cooling load of residences increases substantially for a 3°C rise in standard effective temperature (SET). So, it is essential to control the cooling load consumption in the cities by optimizing the urban morphologies and reducing the UHI intensity. The phenomenon of climate change presents significant obstacles to the energy consumption of buildings, as outdoor weather conditions influence the energy and thermal performance of structures (Huo et al., 2022). To adequately address the issue of climate change, it is imperative to gain a comprehensive understanding of the forthcoming regional and temporal trends in energy use alongside the implementation of energy efficiency measures for building stocks (Deng et al., 2023). Urban Building Energy Models (UBEMs) are derived from Building Energy Models (BEMs), which can analyse energy demand and assess the effects of prospective retrofits on building stock at a city or district level. These models utilize Energy Plus as the simulation engine for analysis and evaluation purposes (Hong et al., 2020). The present study has used UBEMS to investigate the cooling load consumption of residential buildings in complex spatial configurations of a city. Urbanization and population expansion in developing countries have a significant impact on climate change (Parmesan & Yohe, 2003). To analyze the impacts, the urban planners have designed a few schemes. The local climatic zone is one such scheme invented by Oke and Stewart. The local climate zone scheme is a system for classifying urban areas into distinct local climates based on morphological and land cover characteristics (Stewart & Oke, 2012). Several investigators have conducted LCZ classification studies (Alexander & Mills, 2014; Kotharkar & Bagade, 2018; Leconte et al., 2015; Nassar et al., 2016; Skarbit et al., 2017). LCZ classification scheme helps to find the urban morphological patterns of the cities through which researchers can create models for urban energy studies (Cao et al., 2022). The LCZ technique facilitates the classification of spatial configuration within urban areas, which helps to finalize suitable urban designs in the climate change mitigation and adaptation process. The present study has used the LCZ scheme to create urban prototypes to classify complex spatial configurations of the city. Various studies were conducted on the classification of LCZs in different cities. However, most of them are microscale classifications limited to small urban patches. The LCZ classification study conducted in Nagpur indicates that cities with complex urban forms need separate LCZ subcategories. The intra-urban heterogeneity is high in complex urban forms due to unplanned settlement patterns (Kotharkar & Bagade, 2018). Numerous cities in India come under unplanned settlements since their urban morphologies are heterogeneous in nature. The need for classifying the city at the local scale level helps to capture more regional features compared to microscale classification. A multitude of studies have been conducted to examine the correlation between urban form and environmental factors, with the aim of equipping designers and planners with performative indicators that can be utilized during the initial stages of design (Natanian & Auer, 2020). Previous studies have used several classification methods to classify the urban forms and create archetypes to assess performance in terms of energy and microclimate. A study by Joshi et al. (2022) used urban morphological parameters as the independent variable in clustering the urban archetypes. Recent years have seen a rise in studies related to intra-urban heterogeneity in order to enhance urban planning regulations. It is imperative to minimize the number of simulations conducted in these studies during a large-scale calibration process (Deng et al., 2023). Most research has primarily examined the influence of climatic change on the energy efficiency of archetypal or prototype buildings (Deng et al., 2023; Heidelberger & Rakha, 2022; Nagpal et al., 2019; Nik, 2016; Wang et al., 2018;

Yang et al., 2021). However, there is a dearth of comprehensive research on the variations of spatial configuration across the unplanned settlements present in cities, which needs to be adequately elucidated. The complexity of spatial configuration varies for each city, particularly for cities in developing countries where the unplanned settlements are high in ratio, so the division of distinct morphological features is not possible in such cities. To overcome this issue, the current study focuses on an Indian metropolis and presents a detailed process of analyzing the spatial configuration, as well as investigating energy usage for cooling purposes. The study seeks to accomplish two research objectives: (a) To comprehend the spatial geography of the urban area in a highly heterogeneous mixed urban setting. (b) To conduct a quantitative analysis on the spatial configuration of a complex metropolitan area to determine the most efficient urban forms that minimize the energy usage for Air-conditioning. The present study aims to categorize urban prototypes with respect to their energy consumption and analyze them to develop urban planning energy regulation policies.

Research Area

Tiruchirappalli is situated in Tamil Nadu, India, and has a tropical savanna or tropical wet and dry climate, as classified by the Koppen climate classification. Tiruchirappalli is classified as a warm and humid climatic zone according to the National Building Code (NBC-2016). The year is divided into four distinct seasons: winter, which spans the months of January and February, and summer, which encompasses the period from March to June. The monsoon season occurs from June to September, followed by the post-monsoon season from October to December. The city comprises high-rise, midrise and low-rise structures with highly vegetated to bare soil land covers. The city comes under one of the complex-built environments with a mixture of all built-cover and land-cover typologies. The city was chosen for the study for its highly heterogeneous built settings and hot summers. A study by Bhatnagar et al. (2018) indicates that Tiruchirappalli has the highest cooling degree days in India. So, the current study is essential to understand the impact of spatial configuration on cooling load reduction potential.

Methodology

The methodology section is subdivided into five phases as follows.

Phase 1: Sub-classification system

In the initial stage, a novel subclassification system using the Local climatic zones was introduced to segregate the urban morphology into different classes. For classification purpose, we have utilized permutation and combination method to curate different possibilities of spatial configuration with nine LCZ classes (Figure 2).

Phase 2: Model Preparation

Using the sub-classification model, sixty-five different morphologies were obtained (Figure 3). Each morphology was re-arranged into four combinations based on the proportion of land cover and build cover zones (Figure 2b). The LCZ models were configured as per the development control regulations of Tiruchirappalli city. The obtained morphologies and their combinations were modelled in Rhino 7 to export it for simulation.

Phase 3: Image processing

We have used pixel-based segregation (binary classification) in python to find the LCZ classes in the study area. Initially, the training images from the study area of size 40,000 Sq.m were utilized for training the model (Figure 4). The images were converted into two-dimensional binary pixels, and for testing, the high-resolution Google image of the city was divided into numerous urban patches. With the help of a random shuffle, both training and testing binary data were equated to find the LCZ classes of the study area.

Phase 4: Energy Simulation

The model imported from Rhino 7 was used to conduct energy simulation for the study. Rhino 7 helps the researchers as a computational design tool that connects the gap between modelling and simulation (Anton & Tănase, 2016). URBANopt components from ladybug tools are utilized to calculate the cooling load since ladybug is an environmental analysis tool from Grasshopper, which accounts for complex building geometry and weather information (Bajšanski et al., 2024). The standard effective temperature was fixed for all models, which was obtained through a survey of the residents in the city. The model's simulation settings and physical properties are provided in Table 1 and Table 2.

Phase 5: Clustering and Validating

The sixty-five different spatial configurations were clustered through their UMI values using the k means clustering method (Figure 1), and validation was conducted through a one-way ANOVA test. The optimal number of clusters was determined using silhouette scores. The distribution of urban configurations in the clusters was plotted in the area graph and pie-chat for further investigation.

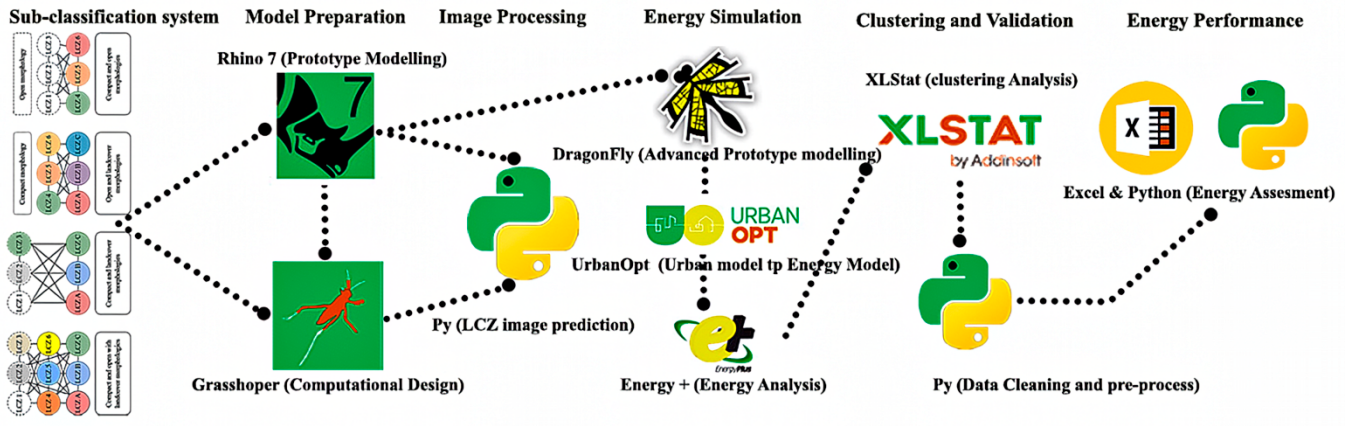

Figure 1. Workflow representation of research phases

Phase 6: Energy performance assessment

In the final stage, the data collected from the URBANopt simulation was analyzed to determine the low-performing built environment present in the city, and the best-performing morphologies were identified and ranked based on their cooling load consumption.

Sub-classification system

A novel subclassification system was introduced in this research for cities that are highly heterogeneous and have complex spatial configurations. This sub-classification helps to capture more complex features compared to the traditional method. A study conducted in China indicates that fine-scale mapping has potential, but we can retain more region-level features from the larger grid size (170 m × 170 m) (Ma et al., 2023). Analyzing a minimal area of 50 m × 50 m is efficient, but large-scale patches are more reliable and efficient for investigating the impact of urban morphological features on building energy consumption. This classification system was created based on the permutation and combination of LCZs (Figure 2a). In this combination, LCZ 7, LCZ 8, LCZ 9, LCZ D, LCZ F and LCZ G were excluded since these LCZs present in the lowest ratio in Tiruchirappalli city. This study aims to cluster the LCZs of an ideal central business district so the most prominent LCZs, which come under compact types (LCZ 1, LCZ 2 and LCZ 3), Open configurations (LCZ 4, LCZ 5 and LCZ 6) and land cover configurations (LCZ A, LCZ B and LCZ C) were chosen for the permutation and combination. In this classification, not more than one land cover was used to define the typology since the study focuses on the energy consumption data of built morphologies.

Model Preparation

Urban blocks are sections of one or more buildings encircled by streets (Schirmer & Axhausen, 2016). The sample city chosen for the model was Tiruchirappalli in South India, which comes under warm and humid climate. The development control regulations of the city were used for the designing of blocks. The minimum plot size allowed for the building was 300 Sq.m., used in the study to create the building blocks (Figure. 2c). Thirty plots were created for one module with a module size of 9000 Sq.m (Figure 2b). Each module was modelled with four different combinations, and the four modules were combined to create one neighbourhood of 38,709 Sq.m. Four combinations of the neighbourhood were designed based on the distribution of morphologies. The first combination has an equal distribution of all morphologies, followed by a 60-20-10 ratio of three zones for the rest of the combinations (Figure 2b). The neighbourhood designed for the study consists of 1200 plots with the distribution of different land cover and built cover types. A block model was designed in Rhino 7 with fixed floor heights for low, mid, and high-rise buildings (Table 1). The number of floors for the low-rise building is 1, the mid-rise building is 3.5, and the high-rise building is 7. The distribution of the buildings in the plot was determined by giving random seed values in the scripting so that for every LCZ, the variations in arrangements of the building block can be achieved. The Final model consisted of 65 zones grouped into six configurations: compact and open with landcover configurations, compact and open configurations, compact with landcover configurations, open with landcover configurations, compact configurations, and open configurations. The open configuration has one zone (LCZ 456), and the compact configuration has one zone (LCZ 123). Compact open with landcover configuration has 27 zones, compact and open configuration has 18 zones, compact with landcover configuration has 9 zones and open with landcover configuration has 9 zones (Figure 3).

Urban Morphology Indicators

Numerous urban morphological indicators (UMIs) have been reported in previous studies, and they are broadly categorized as building block indicators, open space indicators, street indicators, and plot indicators (Elzeni et al., 2022). The selected urban morphology indicators for the current study were Aspect ratio, Sky view factor, Perme-

able surface fraction, Floor area ratio, Height of rough element, Standard deviation of building height, Ground space index and open space ratio. The indicators were selected based on the literature review from published research articles (Apreda et al., 2020; Heris et al., 2020; Palusci et al., 2022; Stewart & Oke, 2012b; Teller & Azar, 2001). These indicators were used in a study conducted in Belgium, where they found that the difference in UMI values between the zones significantly impacts microclimate (Joshi et al., 2022). The urban district model from the Dragonfly was used to calculate the UMI values. The formulas used to calculate the indicator values are given in Figure 2d. In the correlation matrix we found that OSR (Open space ratio) was highly co-relating with Permeable surface fraction and Ground space index, so it was not used for the clustering process since it would alter its results Figure 5.

Image Processing

The area of Tiruchirappalli city constitutes 167.2 Sq.km, of which 8 Sq.km was taken for study from the region of KK Nagar zone (Figure 4d). The city was divided into five zones for administrative purposes and KK Nagar is populated high compared to other zones (Figure 4c) (Karthik, 2021). To conduct image classification, the study area was divided into urban grids with two fixed grid sizes, one larger (400m × 400m) and another smaller (200m × 200m). High-resolution Google map images of the identified LCZs in the city were fed as input to the image classifier model. The images were converted to the binary matrix, and the values were reshuffled multiple times to train the model for every probability. Ultimately, the Python program was utilised to determine the appropriate zone for the test data, which consisted of Google photos measuring 200m x 200m. Each smaller grid (200m × 200m) comprises three different morphologies, which were difficult to process through the GIS model and prone to errors while calculating for a large area. This approach provides a comprehensive understanding of the morphology distribution with higher accuracy. The method to convert the Google images into binary matrices is given in Figure 4a. For each LCZ class, 10 images from the study area were used to train the model for classification. A total of 650 images were used to train the model, and their binary data were collected to classify the test images, as shown in Figure 4d.

Simulation

The energy simulation method used in this study was divided into three sub-stages: (a) Importing the urban models, (b) Energy plus weather file generation from UWG (Urban weather generator) for all urban prototypes, (c) Cooling load calculation Figure 1. The energy plus weather file (city code: 433440) was obtained from climate.onebuilding.org website under WMO Region 2. By modelling the LCZs in the Urban Weather Generator (UWG), EPW data were collected for all 65 prototypes. Using meteorological data from the rural weather station, UWG generates a new urban EPW file and determines the hourly air temperature and humidity within the urban canopy. The article by Bueno et al. (2014) describes the workflow and the four UWG modules. The evaluation of the UWG against field data from Basel, Switzerland, and Toulouse, France, has yielded satisfactory results (Bueno et al., 2013). Generally, urban energy evaluation is conducted through statistical data, physical models, and degree days (Li et al., 2021). The physical model method has high accuracy in calculating energy data when compared with the other two methods (Chen et al., 2018). The influence of the microclimate in the cooling load can be calculated with better accuracy in simulation models (Li et al., 2021). The district cooling load of the LCZ was obtained from the URBANopt component through the geoJSON file. Dragonfly was used to calculate the district cooling load data by converting the simulation model into a geoJSON file. The blocks in the urban prototypes were divided into seven zones (Z1-Foyer, Z2 - Guest room, Z3 - Office space, Z4 - Living room, Z5 - Pantry, Z6 - Bed Room, Z7 - Bath and Z8 - Bed Room) (Figure 2c). Zone 6 and Zone 8 were fixed as air-conditioned space for the simulation. The model's simulation settings and physical parameters were presented in Table 1 and Table 2, adapted from (Kolhatkar et al., 2022).

Table 1. Building Properties

Properties		Inputs
Floor height	All floors	4 m
No of Floors	Low, Mid and High	1, 3.5 and 7
Wall thickness		0.23 m
Construction Type	Bricks and Concrete	
U-Value of wall	For all the Zones	0.38 W/Sq.m. K
U-Value of roof		0.25 W/Sq.m. K
U -Value of glazing		2.60 W/Sq.m. K
WWR		0.25 (All directions)
SHGC of glazing		0.65
Air-conditioned zones	65 Prototypes	Zone 6 and Zone 8

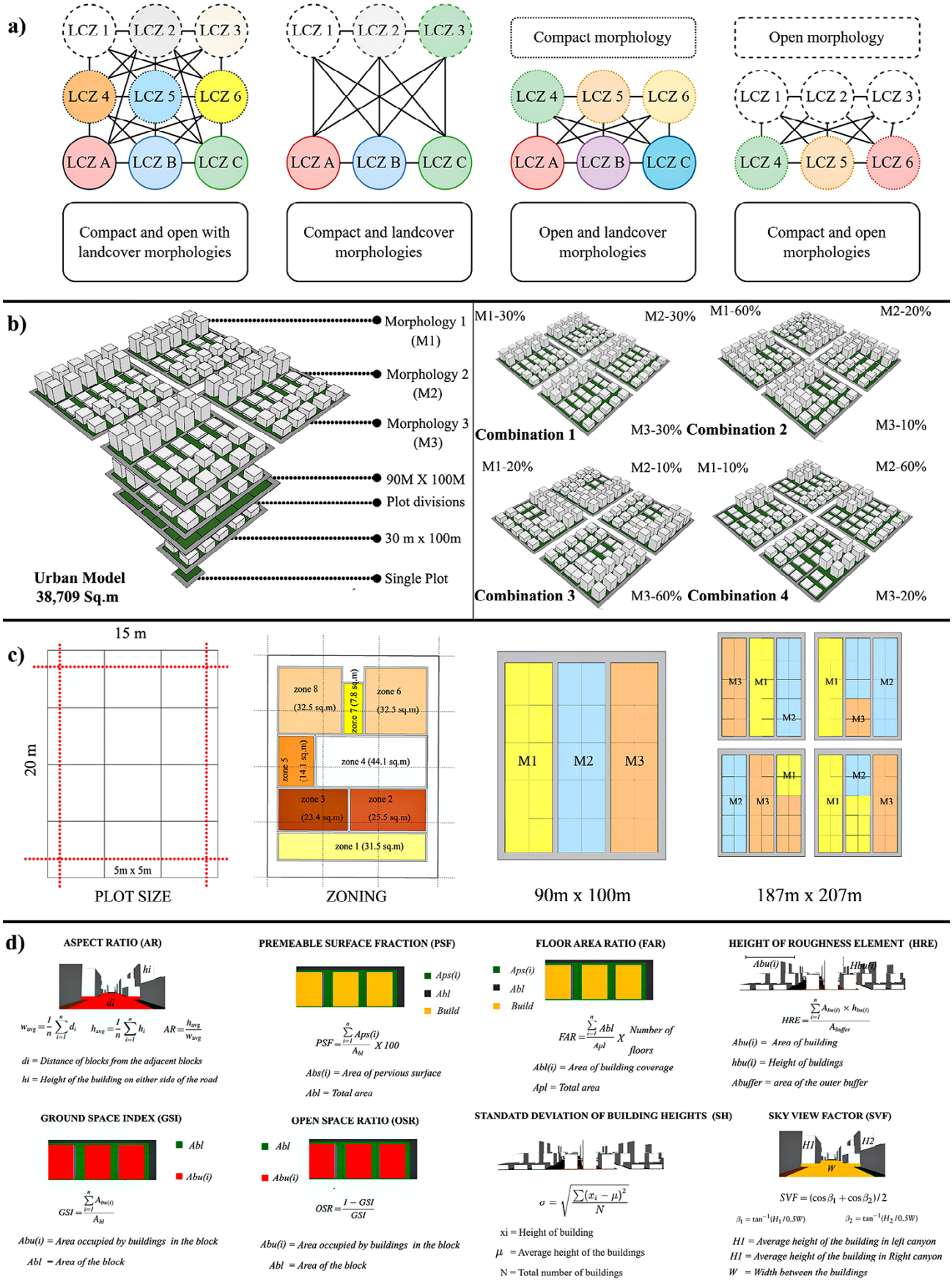

Figure 2. Prototype classification through LCZ method a) Sub-classification system b) Urban morphology model c) Model preparation method d) Urban morphology indicators

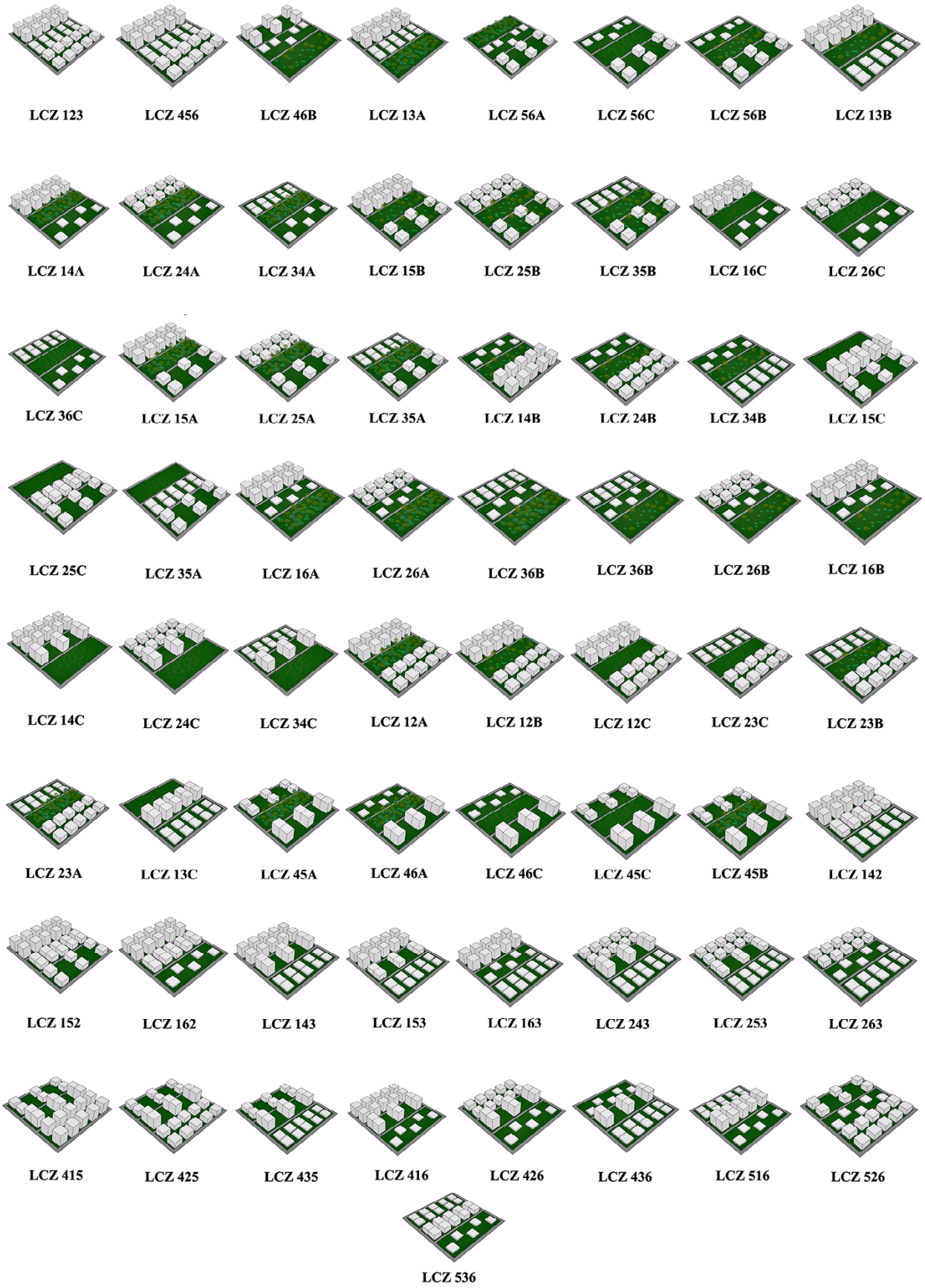

Figure 3. Urban prototypes of local climatic zones

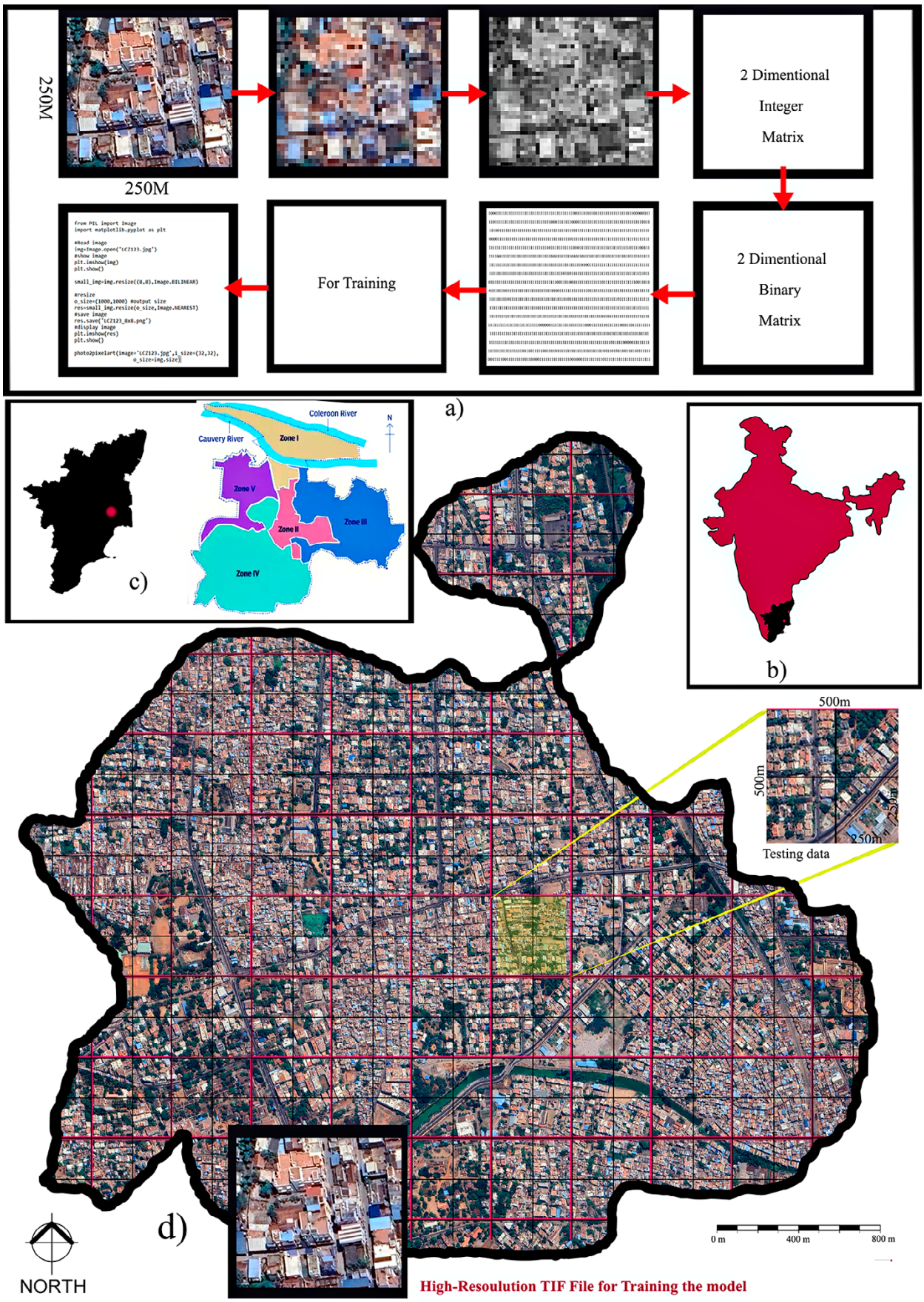

Figure 4. Mapping method (a) Image processing method (b) Map of Tamil Nadu state in India (c) Map of Tiruchirappalli city (KK Nagar) (d) Satellite image of the study area

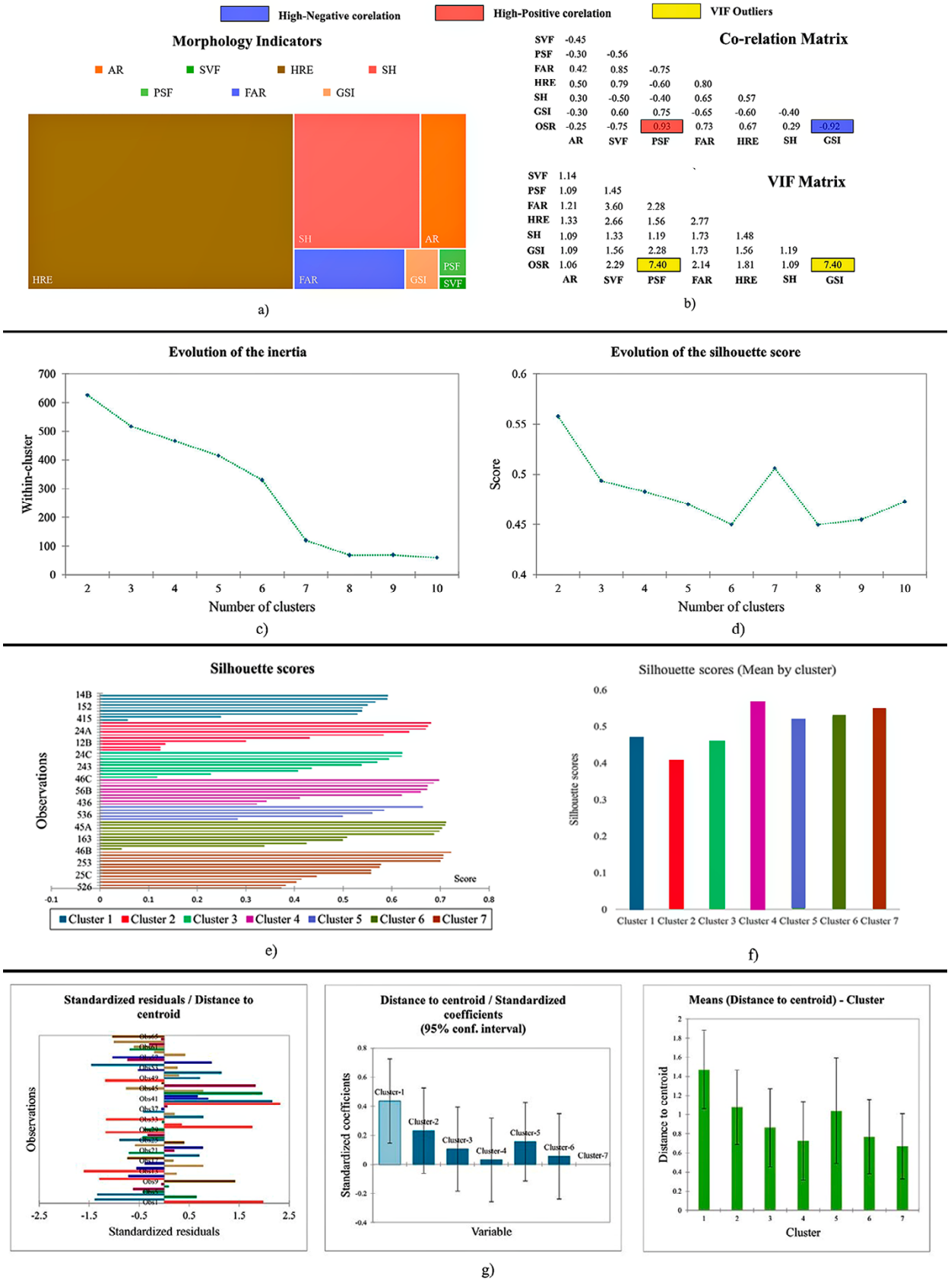

Figure 5. Clustering Results (a) UMIs (b) Co-relation and VIF Matrix of UMIs (c) Inertia values (d) Silhouette scores (e) Individual silhouette scores (f) Distance from the average silhouette scores (Clusters) (g) ANOVA Results

Table 2. Simulation settings

UWG parameters		Inputs
Building program	Midrise Apartment's	
ASHRAE Climate zone	2 - Hot	
Building Age	1980 - 2004	
Construction Type	(Mass) Bricks and Concrete	
Urban Patch size	210 M X 210 M	
Boundary conditions	UBL at Daytime	1000 m
	UBL at Nighttime	450 m
	Inversion height	200 m
Previous Layer	Thickness	0.95
	Conductivity	1 W/m-K
	Volumetric heat capacity	1.6e6 J/cu.m-k
Impervious layer	Thickness	0.95
	Conductivity	1 W/m-K
	Volumetric heat capacity	1.6e6 J/cu.m-k
Anthropogenic Heat capacity	Same for all Zones	4 W/Sq.m
Occupation Schedule	Midrise_Appartment_Occ	
Simulation Period	Summer (1st -Mar – 31st May) TMY	
Set Temperature	Based on the survey taken from residents	26.3°C (Summer)

Clustering and Validation

An unsupervised machine learning method (K-means) was used in this study, which groups the n observation into k clusters. It starts with a predetermined number of clusters (k) and n data points; the algorithm chooses cluster centres randomly. In this method, data points are categorized according to the closest cluster centre, and the process is achieved by minimizing the sum of square distances between any data point and its closest cluster centre within the cluster, as indicated by the equation presented in Jain (2010). Generally, the centroids are chosen randomly by the K-means algorithm. To avoid this, we have employed the centroid initialization technique known as k-means initialization to avoid the random selection of centroids. The most optimal initial centroid was chosen using this method, and the XLSTAT tool was used for this process. Many different approaches have been used to determine the number of clusters. For clustering analyzes, finding the ideal number of clusters is essential to avoid errors in the clustering process. For this research, we used the silhouette score method, which calculates an overall representative score to test the effectiveness of the clustering. It works based on the compactness of individual clusters (intra-cluster distance) and the separation between clusters (inter-cluster distance) as given in equation 1.

$$si = \frac{bi - ai}{max(bi, ai)} \tag{1}$$

ANOVA and MANCOVA are the primary criteria for validating previous studies' clustering results (Panuwatwanich & Nguyen, 2017). For the external criterion analysis, we selected the average air temperature (Ta) of the LCZs as the dependent variable. The external variable in this study cannot be a factor influencing or providing information about urban morphology indicators. One-way ANOVA was used in several studies to validate the results of clustering analyses. So, one-way ANOVA is utilized to confirm the clustering results by finding whether the mean air temperature (Ta) fluctuates among the clusters.

Results and Discussion

Validating the clustering results

It is essential to determine the suitable number of clusters for the k means in the clustering algorithm. Unlike the hierarchical clustering method, k means cannot independently determine the number of clusters. The silhouette score method was used to fix the final number of clusters. The maximum value of the cluster was fixed as 10 (k) since increasing the k value decreases the inertia within the cluster (Figure 5). In various studies Silhouette score helps to find the effectiveness of the clustering algorithm. In the evolution of the silhouette score, a sharp rise was observed at k=7 (Figure 5d). In contrast, the inertia score steeply decreases at k=7, near 100 (Figure 5c). There was no significant decrease in the inertia level after 7, from which the results concluded that the data can be divided into 7 clusters (Table 2). The average silhouette score was 0.475; Figure 5e denotes that a significant number of individual silhouette score were higher than the average, which explains that the clustering algorithm was well performed. To validate the clustering results, one-way ANOVA was used in this research. Figure 5g demonstrates the distance of the air temperature data from the centroid for all prototypes. The research concludes that there is a significant amount of deviation between the data with a 95% confidence interval. The specifics of the ANOVA test are denoted in Table 4 and Table 5.

Analyzing the clustering results.

Seven Groups (G1-G7) were acquired through clustering results. Cluster 5 has the lowest number of zones (Z=5), while Cluster 7 has the highest number of zones (Z=13) (Table 6). The zones deprived of land cover were grouped along with those with land cover configurations. low-rise configurations were grouped along with the high-rise. The combination of open configurations and compact configurations was found in G6 and G7. Since the intra-cluster difference is less than the inter-cluster difference, the clustering results were fit to further analyze (Table 7). Aspect ratio (AR), Sky view factor (SVF), Height of roughness element (HRE), Stand deviation of building height (SH), Permeable surface fraction (PSF), Floor area ratio ((FAR), Ground space index (GSI) and Urban district cooling load (UDCL) were the variables used for the cluster analysis. The highest aspect ratio and lowest sky view factor were found in compact and open built with landcover configurations and compactly built configurations. The height of the roughness element (HRE) and Standard deviation of building heights (SH) were high in compact-built forms and low in open-built forms. The values of the PSF were between 0.2 and 0.4, which shows that the mixed morphologies were similar in the distribution of permeable surfaces. The GSI values were high in compact-built configurations compared to open-built configurations, and a distinct difference was seen between the configurations with land cover and those deprived of land cover. The floor area ratio was high in LCZ 142 (Compact high rise and mid-rise with open high-rise category) and low in LCZ 36A (Compact low rise and open low rise with dense trees category). The clustering results indicate that unrelated mixed spatial configurations can be grouped due to the similarities in the distribution of the classes. Thus, it explains that when dealing with complex urban forms, larger grid sizes are essential to capture the regional geographical features of the city.

Inter-cluster variation

The clustering results indicated that 65 typologies can be clustered into seven groups (G1-G7). The minimum and maximum distance between the cluster centroids were 2.4 and 18.9 (Table 7). Among all the groups, G1 has high AR, HR, FAR and SH due to the distribution of morphologies within the group (Figure 6a & Figure 7). Similarly, G1 has a high urban cooling load (284.13 Gjs) in summer, and 40% of the zones in G1 come under compact with open-built con-

Table 3. Numbers of Iterated clusters

Clusters	C1	C2	C3	C4	C5	C6	C7	C8	C9
Silhouette scores	0.56	0.49	0.47	0.46	0.45	0.52	0.45	0.46	0.47
No of clusters	k=2	k=3	k=4	k=5	k=6	k=7	k=8	k=9	k=10

Table 4. ANOVA Results

Source	DF	Sum of squares	Mean squares	F	Pr > F
Model	9.000	5.266	0.585	2.343	0.026

Table 5. Cluster centroid data.

Variable	Obs. with missing data	Obs. without missing data	Minimum	Maximum	Mean	Std. deviation
Distance to centroid	0	65	0.000	2.495	0.792	0.545

Table 6. Clustering Result

Cluster	G1	G2	G3	G4	G5	G6	G7
Number of objects by cluster	9	10	9	9	5	10	13
Within-cluster variance	3.414	1.891	1.107	0.801	1.706	0.862	0.609
Minimum distance to centroid	0.487	0.185	0.433	0.277	0.408	0.137	0.053
Average distance to centroid	1.471	1.078	0.862	0.725	1.040	0.767	0.668
Maximum distance to centroid	2.890	2.402	2.062	1.841	1.908	1.346	1.143
Urban Prototypes	14A	24A	34A	35B	36C	25A	35A
	15A	15B	25B	26C	35C	24B	34B
	14B	16A	16C	36A	36B	15C	25C
	123	14C	26A	34C	536	16B	26B
	142	153	24C	263	56C	163	253
	143	162	456	436		516	526
	152	416	243	23C		425	435
	415	13A	426	46C		13B	23A
	12A	12B	46A	56B		13C	23B
		12C				45A	45B
							45C
							46B
							56A

figuration. G1 has low SVF and GSI due to the distribution of fewer landcover zones within the cluster. G2 has high GSI and low FAR since 40 % of them were compact low and mid-rise configurations (Figure 6b & Figure 8). The difference in the PSF between the groups was insignificant due to repetitive urban prototypes. The difference between G3 and G5 was also insignificant due to the distribution of similar morphologies in the groups except the open-built type, which was present for 15% (Figure 6b). Similarly, G4 and G7 have low differences, which can be comprehended by the difference between the centroids (Table 7). The GSI was similar between the groups except for G2 since it was the only cluster with fewer land cover types. G1 and G5 have high differences in the values of the variables selected for the clustering. Similarly, G4 and G1 have high dissimilarities when compared with other groups. Open-built type was present only in G3, and compact-built morphology only in G1. The difference between the centroids of G1 and G3 proves that the clusters were separated far from each other (Table 8). Similarly, the G2 and G5 clusters were separated far from each other, which can be understood by the distribution of cluster centroids. Compact with open built and land cover typology has maximum share with G5 (70%) and G1 (30%). The results conclude that the variations between the clusters were due to the distribution of urban morphology within the spatial arrangements. The current study provides a novel approach in LCZ modelling for complex city forms, and using this approach, researchers can benefit by finding suitable morphology for the cities under warm and humid climate. This study also helps to create morphological clusters for the cities to research the distribution of UHI in different clusters.

Table 7. Distance between the cluster centroids

Clusters	G1	G2	G3	G4	G5	G6	G7
G1	0						
G2	4.013	0					
G3	10.088	6.078	0				
G4	15.417	11.405	5.335	0			
G5	18.989	14.977	8.908	3.574	0		
G6	7.328	3.319	2.761	8.093	11.666	0	
G7	13.023	9.011	2.938	2.397	5.971	5.697	0

Table 8. Variation between and within the clusters

Variation inertia	Absolute	Percent
Within-cluster	81.473	3.75%
Between-clusters	2089.268	96.25%
Total inertia	2170.741	100.00%

Identified LCZs in the Research area

The study area was divided into 195 urban patches using 200 m x 200 m grids. Each urban patch was tested through image classification model in Python by randomly generating the images. Out of 195 urban patches, 15 images were not able to be classified due to the absence of build cover configurations. 180 images were classified successfully, and their representative groups were provided in Figure 9a. G5 and G6 were in small ratios with LCZ 56C, LCZ 45A and LCZ 13B configurations. Similarly, G1 and G3 were distributed for 15% of the study area. LCZ 34A and LCZ 12A were the configurations under the G1 and G3. 32.2% of the distribution was under G7 and 34.4% under G2 (Figure 9b). The confusion matrix of the group indicates the image classification accuracy was high in G2, G7 and G4 since they share 80.4% of the study area. The precision, recall and F1 scores of the 3 groups are given in Table 9. LCZ 12A, LCZ 12B, LCZ 12C, LCZ 13A, LCZ 416, LCZ 153, LCZ 34A, LCZ 35B, LCZ 23C, LCZ 34C, LCZ 56C, LCZ 45A, LCZ 13B, LCZ 53A, LCZ 23A, LCZ 45B, LCZ 23B and LCZ 56A were present in the study area (Figure 10a). The morphology characters of the classified urban patches were extracted and co-related with the UMI values of Urban prototypes. For validation, 18 LCZ configurations in the study area were compared with their urban prototypes. The RMSE values for the respective indicators are given in Figure 10b. The classification results conclude that 90% of the study area has configurations with dense and scattered trees. The presence of open high-rise and compact high-rise urban configurations was less than 7%. The confusion matrix presented in Figure 10c denotes the total number of images classified accurately under each group.

Table 9. Classification validation table

Groups	Precision	Recall	F1-score
Group 2	82.85%	85.51%	84.91%
Group 7	88.50%	83.79%	85.32%
Group 4	55.82%	59.37%	56.63%

Energy Performance Investigation

Investigation of energy performance was conducted through 2 objectives: (a) analyzing the cooling load consumption for all combinations of 65 zones and (b) Analyzing and ranking the performance of the classified spatial configurations present in the city. The cooling load consumption for each LCZ was calculated through a simulation model in URBANopt. The SET temperature was fixed constant for all zones so that the results could be compared without deviation of occupant's behaviour. The heat map of the energy consumption is shown in Figure 11e. The spatial configurations deprived of vegetation have higher energy consumption than other types of configurations. Compared to other zones, open high-rise configurations and compact high-rise configurations with dense trees consume high energy for cooling the indoor spaces. Compact midrise configurations and compact low-rise configurations (23A, 23B and 23C) consume less than open morphologies in a few combinations (Figure 11a). Densely vegetated configurations like 15A and 14B classes reflect high variation in the energy consumption between the combinations. The impact of vegetation in reducing the cooling load was significantly low in high-rise zones compared to low-rise zones. Open configuration with a combination of compact configurations consumes high energy when there is a lack of dense or scattered trees. Further analyzes were conducted on the morphologies present in the city. The simulated data were plotted against the real-time cooling energy data to validate the urban prototype model. TNEB (Tamil Nadu Electricity Board) data were used to calculate the rest time cooling load for the buildings. The RMSE value was 0.55, and all 18 morphologies were used for the validation (Figure 11c). The distribution of the groups was analysed and mapped in Figure 11. We found that approximately G2, G4 and G7 were present in over 80% of the study area. So, the study was further conducted by analyzing of the morphologies in G2, G4 and G7. LCZ 416 (open high rise and compact high rise with open low-rise zones) consume high energy for cooling the spaces. Combination 2, which is 60% of the first class, 20% of the second class, and 10% of the third class, has high cooling load consumption in most morphologies. The lowest cooling was found at 23C (compact mid-rise and low-rise with shrubs), which is 150GJs. The morphologies in Group 2 consume a high cooling load when compared with Group 4 and Group 7 (Figure 11d).

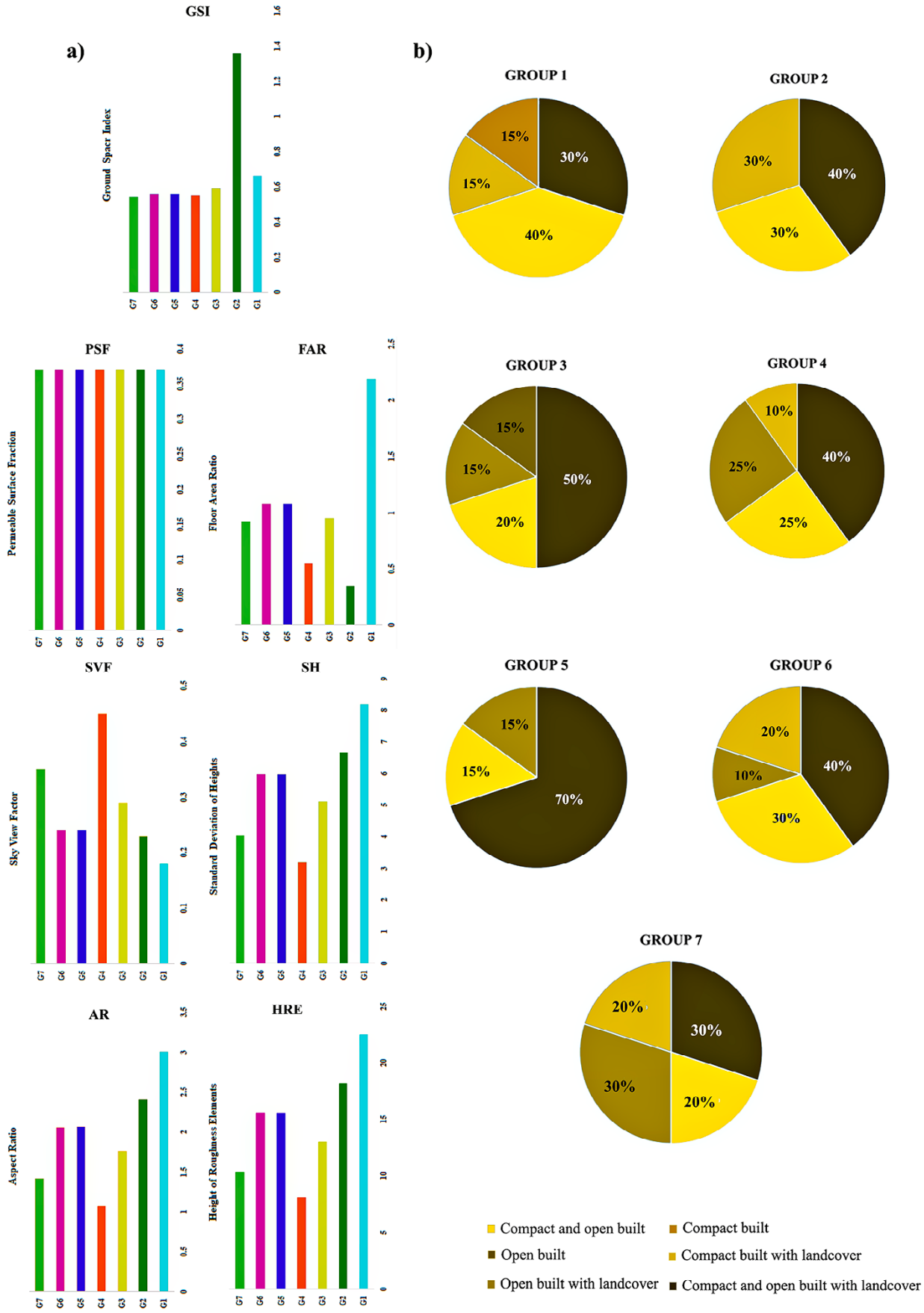

Figure 6. LCZ graphs (a) UMI values for each group (b) LCZ distribution for each group

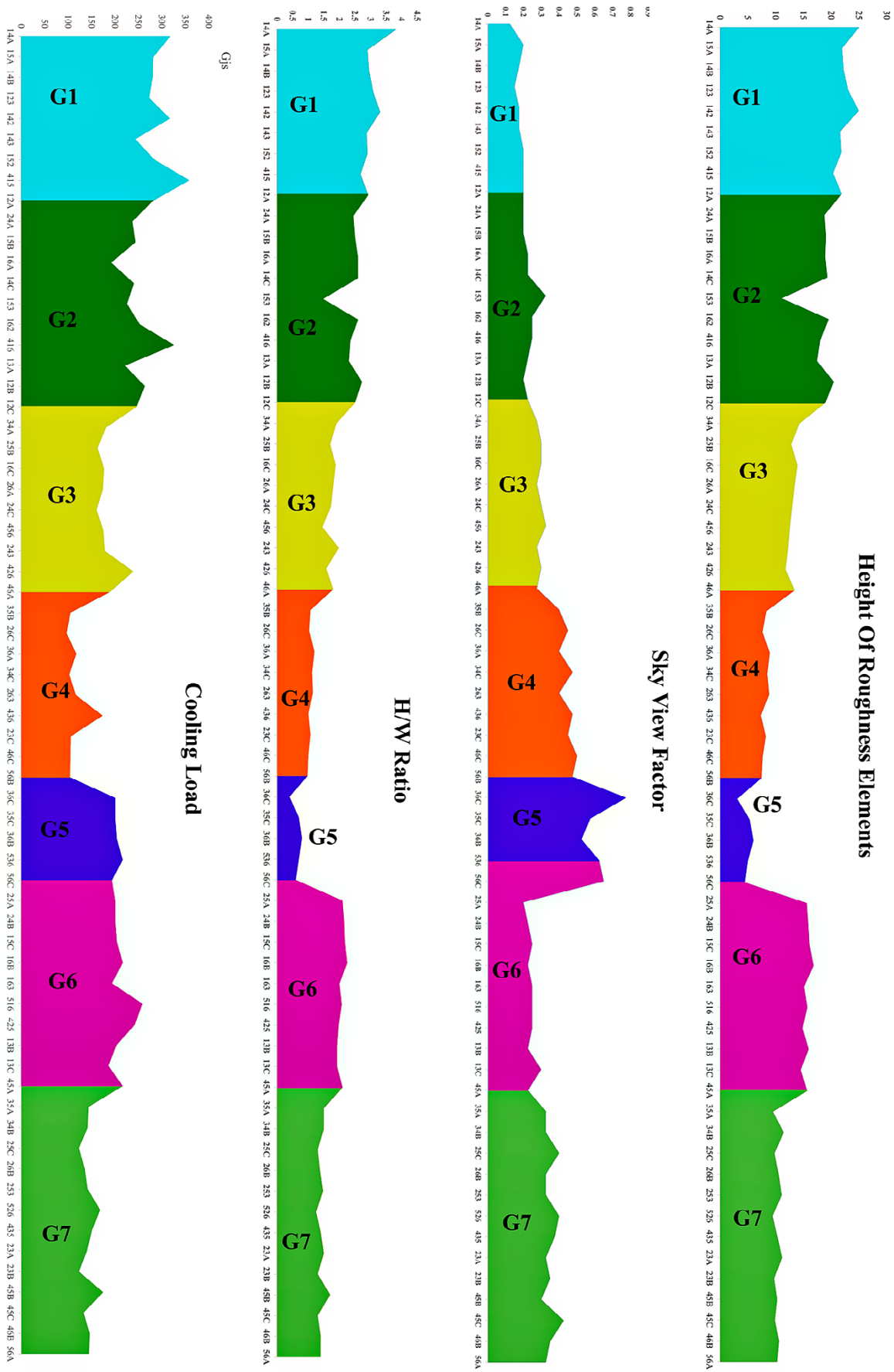

Figure 7. UMI values of urban prototypes

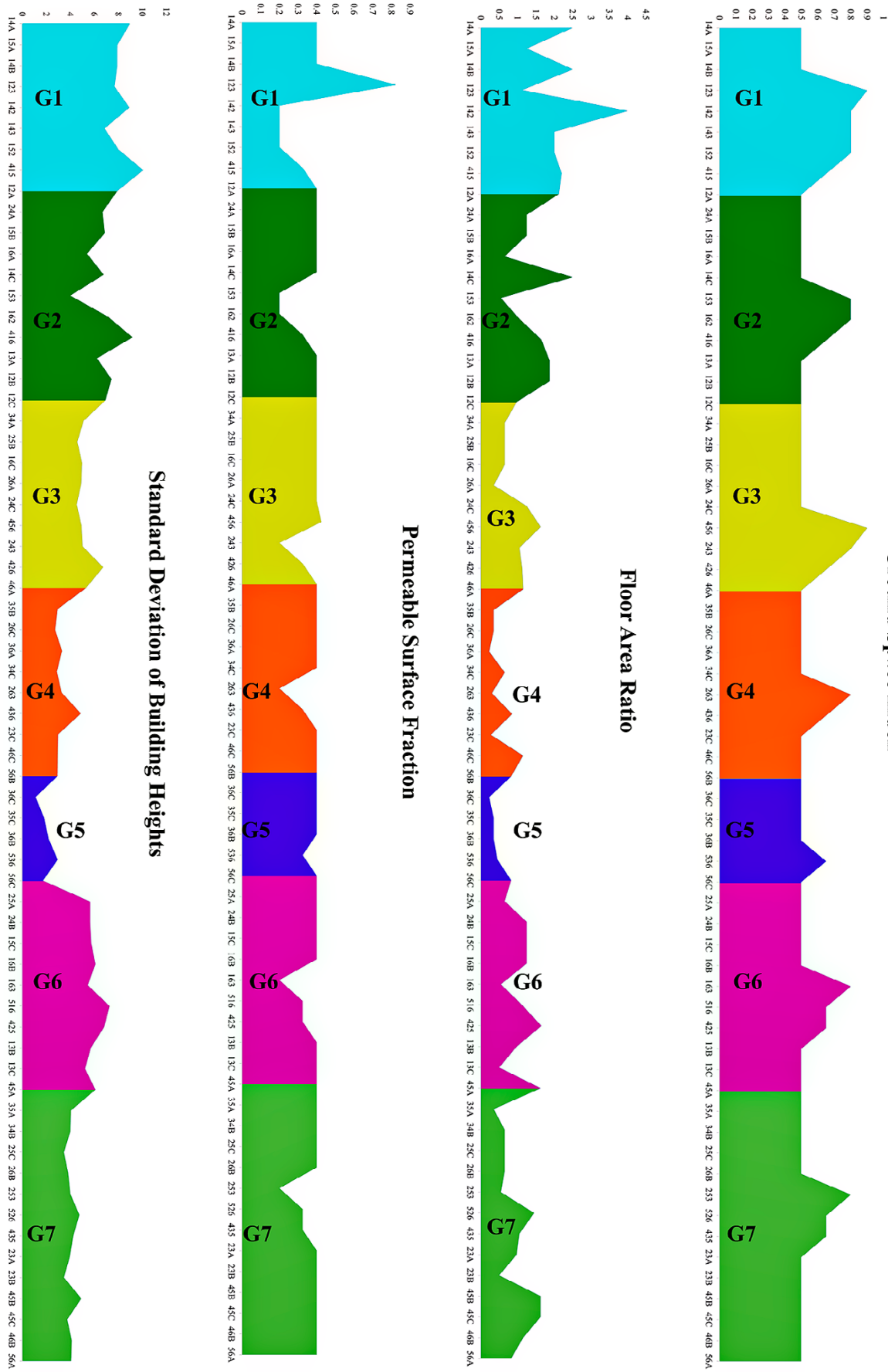

Figure 8. UMI values of urban prototypes

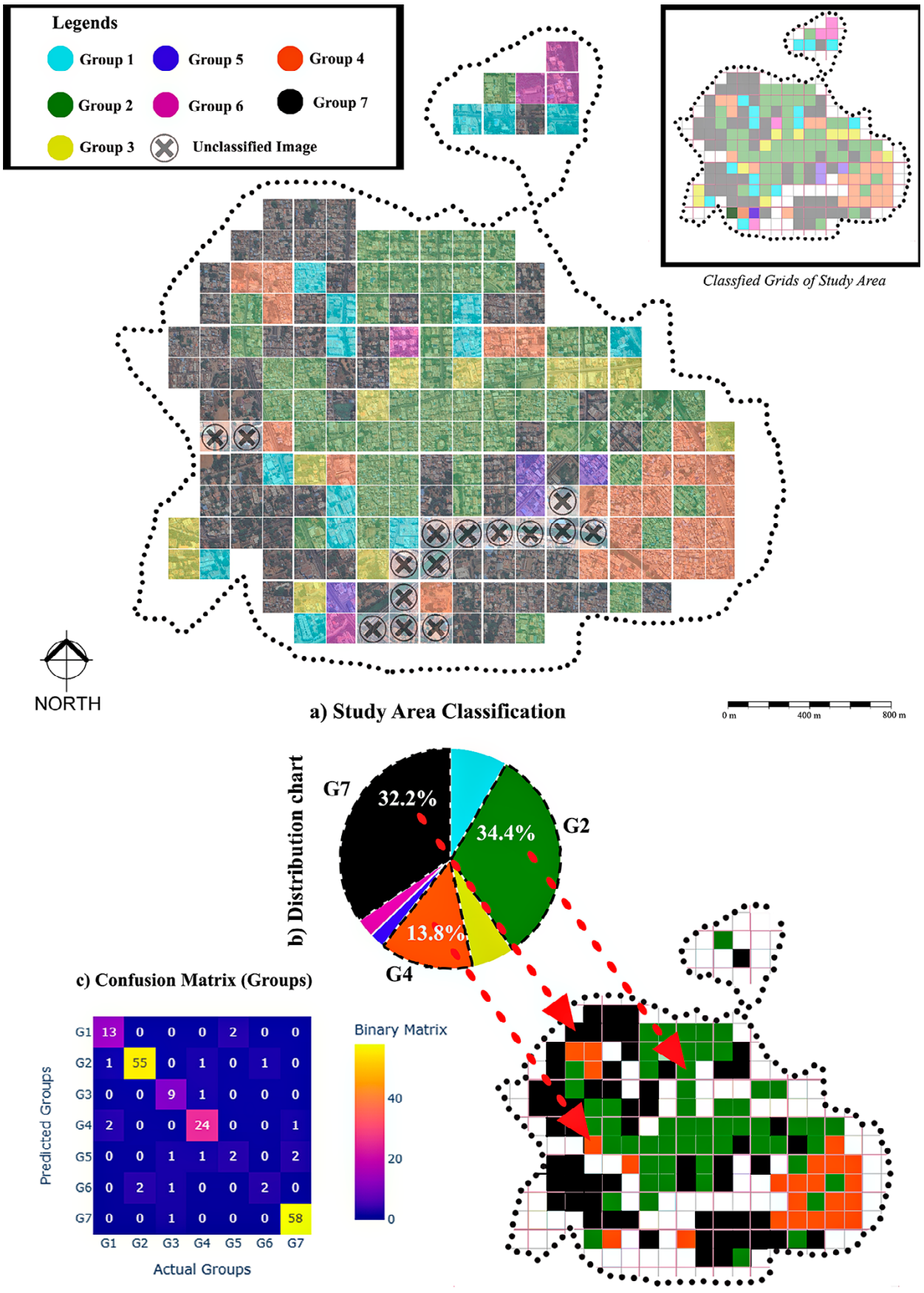

Figure 9. Study area classification results (a) Classification map (b)Distribution of groups in the study area (c) Confusion Matrix of image classification (Groups)

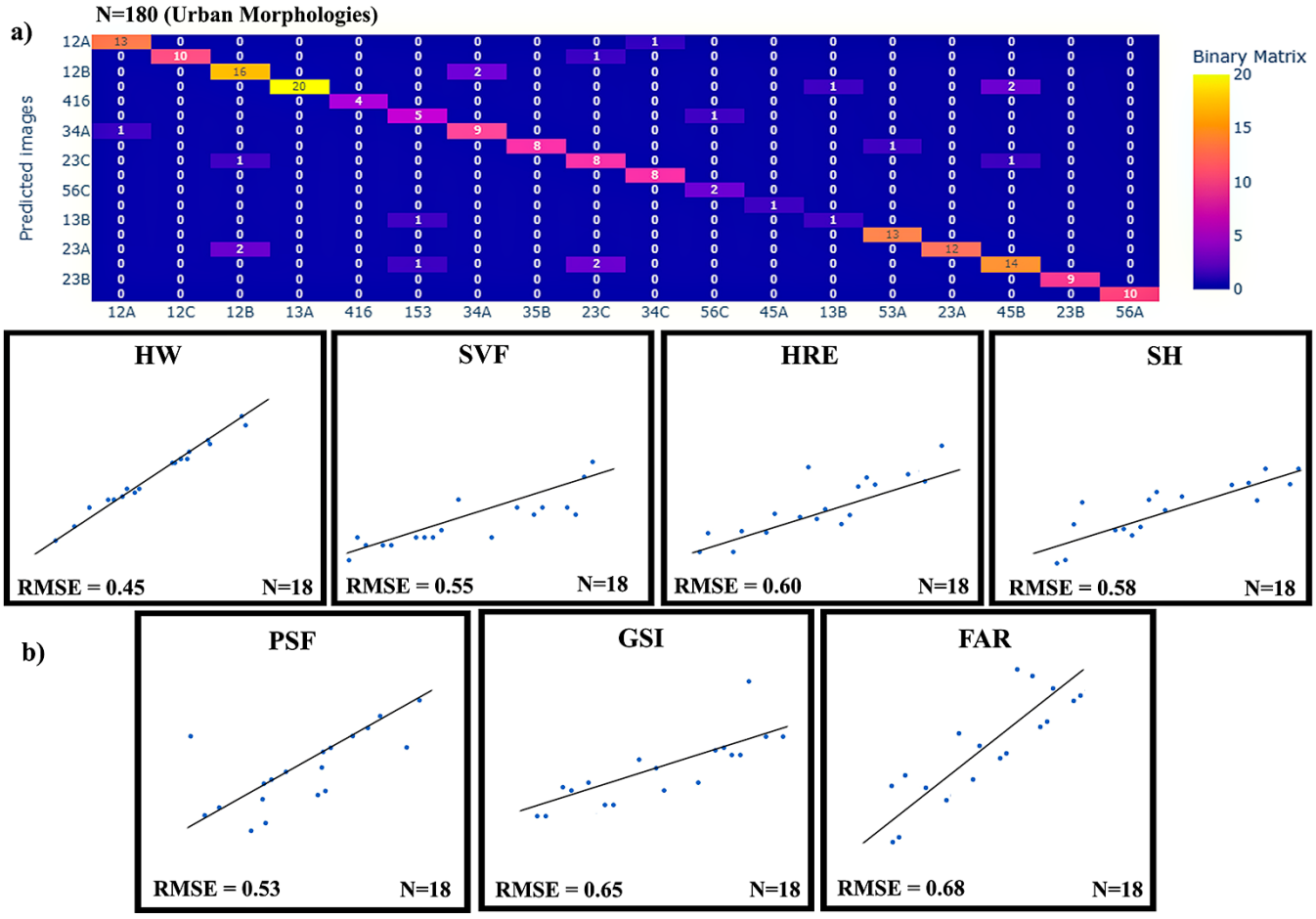

Figure 10. Study area classification results (a) Confusion matrix of classified images (b) RMSE values for validating the urban prototypes

Conclusion

The current study takes KK Nagar in Tiruchirappalli as an example and analyzes the impact of urban spatial geography on the air-conditioning energy usage. In this study, we have proposed a novel method for classifying the city using a two-layer subclassification system. Since major Indian cities are unplanned settlements with more than two LCZ in a grid size of 0.25 sq. km, this study helps classify the highly heterogeneous morphology in cities. The gird size chosen to create the morphology was 38,709 Sq.m. Through this extensive grid size, we can retain more regional geographical features of the city compared to using smaller grids. The research intends to concentrate on the complex urban forms which were not addressed in previous studies to the best of our knowledge. Urban morphology significantly influences the energy consumption of buildings, resulting in a reduction in cooling load Javanroodi et al. (2018). The results of the current study support Javanroodi et al. (2018) statement. The impact of mixed morphologies on energy consumption differed from the planned cities. Compared to the other studies on the impact of urban forms on energy consumption, this research makes a significant contribution in explaining the complex urban structures and their impact on cooling energy consumption. For urban planning, we have found that emphasizing the urban morphology layouts and green cover ratios, such as dense trees (Highly vegetated), Scattered trees (sparsely vegetated) and shrubs (lowly vegetated), is crucial in determining the cooling load consumption in a compact mid-rise and open low-rise morphologies with lands covers. These findings provide insights to urban planners and designers in reducing the energy taken for cooling indoor spaces in mixed morphologies. In policy development, our research can serve as a reference for policymakers. For instance, identifying high energy-consuming urban patches and installing PV panels to reduce the on-grid energy usage. Furthermore, our research demonstrated a workflow for classifying the city morphologies into clusters based on their spatial characteristics. It is worth noting that previous studies have explored the impact of urban morphology on cooling loads, including a study conducted by Kotharkar et al. (2022) in which the author explains that lower cooling loads were seen in open morphologies

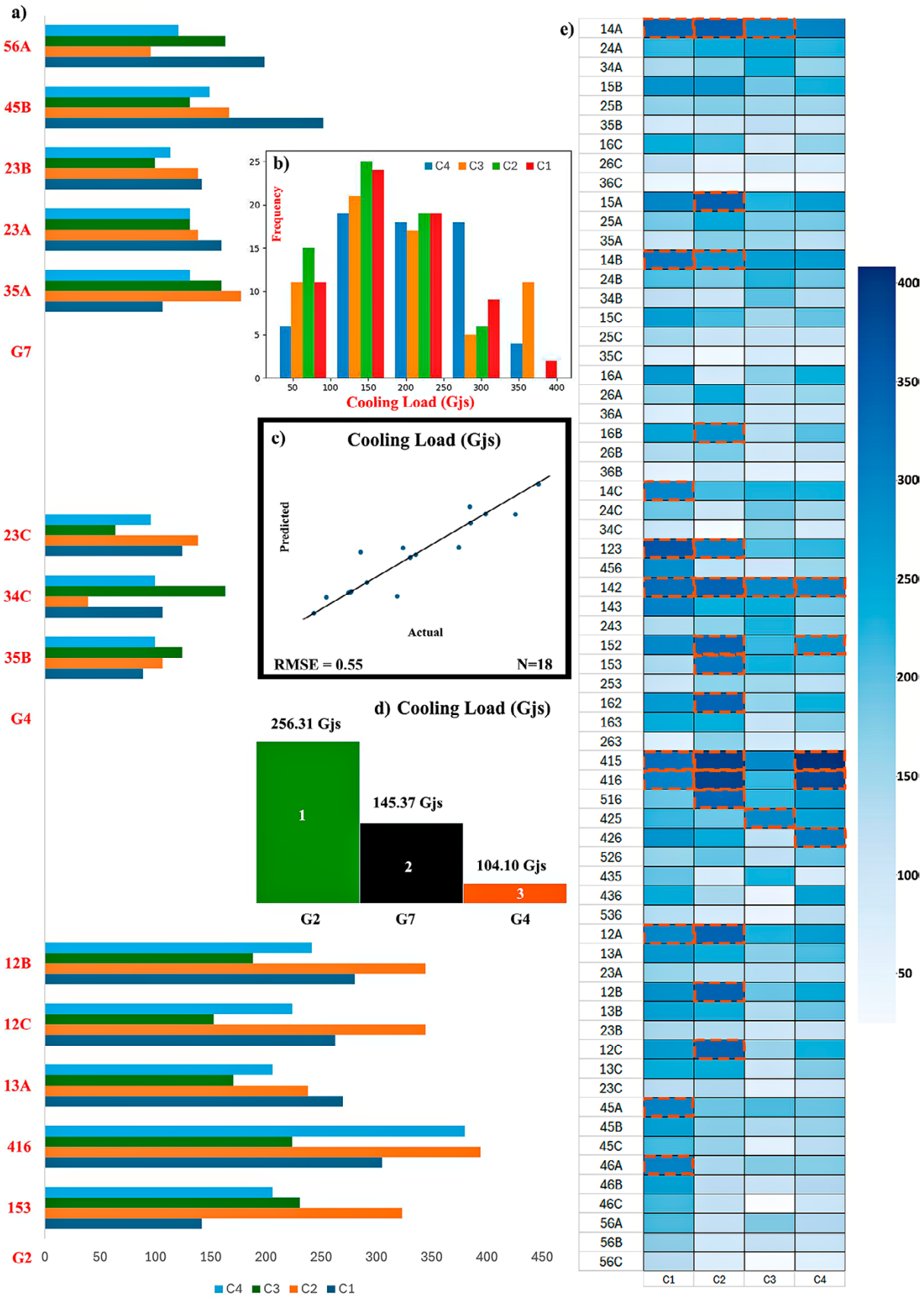

Figure 11. Energy simulation results (a) Cooling load of city LCZs (b) Frequency of cooling loads (c) RMSE values for predicted and actual energy (d) Ranking of groups based on the cooling loads (e) Cooling loads Heat map for all urban prototypes

with high vegetation cover. Similarly, a study conducted in China shows that low and medium-rise structures use more energy for cooling and explains that compact mid-rise configuration's cooling demands were higher than open high-rise (Yang et al., 2022). This study identifies the intricate details in urban morphology at the neighborhood scale through the comparative analysis of different LCZs. It was found that the impact of vegetation on cooling energy consumption of open and compact high-rise along with mid-rise configuration is low. It also explains that increasing the green cover ratio will not help in reducing energy consumption for mixed high and mid-rise morphologies. This study is limited only to residential buildings and hotels, and the results will not be applicable to commercial or office buildings with 8-hour operation slots. There is a scope for future research in studying the arrangement pattern of the buildings and its impact on the reduction of heating loads in cold regions.

The important results of our investigation are as follows:

a) An innovative method for categorizing the complex urban structure of a city. The findings provide valuable design for urban planners and energy policymakers seeking to decrease cooling energy consumption through form-based codes. Our classification approach can be used to classify the morphologies for other cities in future research. This study provides broad insights into sustainable urban development worldwide.
b) In the study area, LCZ 23C (Compact mid-rise and low-rise with sparse vegetation), 34C (Compact low-rise and open high-rise with sparse vegetation) and 35B (Compact low-rise and open mid-rise with scattered vegetation) urban forms needed less energy for air-conditioning in residential neighborhood. The intervention of open or compact low rise in the mixed morphologies reduces the cooling energy consumption drastically.
c) The high frequency of cooling load was between 150Gjs to 200Gjs in the city (Figure 11b). It indicates that the cooling load reduction potential is high in the city when compared to the study area of Nagpur, which was researched by Kotharkar et al. (2022)
d) The Open and compact high-rise with low-rise structures consumes high cooling energy (>400Gjs), which indicates that the high-rise structures with open low-rise combinations are not suitable for warm and humid climate conditions.

Acknowledgement

We are grateful to our institute for providing valuable data and time, inspiring us to complete our research successfully.

References

Abougendia, S. M. (2023). Investigating surface UHI using local climate zones (LCZs), the case study of Cairo's River Islands. *Alexandria Engineering Journal*, 77, 293–307. https://doi.org/10.1016/j.aej.2023.06.071

Alcoforado, M. J., Lopes, A., Alves, E. D. L., & Canário, P. (2014). Lisbon Heat Island. *Finisterra*, 49(98), 61–80.

Alexander, P. J., & Mills, G. (2014). Local climate classification and Dublin's urban heat island. *Atmosphere*, 5(4), 755–774. https://doi.org/10.3390/atmos5040755

Anton, I., & Tănase, D. (2016). Informed Geometries. Parametric Modelling and Energy Analysis in Early Stages of Design. *Energy Procedia*, 85, 9–16. https://doi.org/10.1016/j.egypro.2015.12.269

Apreda, C., Reder, A., & Mercogliano, P. (2020). Urban morphology parameterization for assessing the effects of housing blocks layouts on air temperature in the Euro-Mediterranean context. *Energy and Buildings*, 223, 110171. https://doi.org/10.1016/j.enbuild.2020.110171

Arnfield, A. J. (2003). Two decades of urban climate research: A review of turbulence, exchanges of energy and water, and the urban heat island. *International Journal of Climatology*, 23(1), 1–26. https://doi.org/10.1002/joc.859

Bajšanski, I., Stojaković, V., Tepavčević, B., & Jovanović, M. (2024). A parametric approach for evaluating solar panel insolation in urban areas: Courtyard design case study. *Geographica Pannonica*, 28(2), 115–130. https://doi.org/10.5937/gp28-50098

Barrao, S., Serrano-Notivoli, R., Cuadrat, J. M., Tejedor, E., & Saz Sánchez, M. A. (2022). Characterization of the UHI in Zaragoza (Spain) using a quality-controlled hourly sensor-based urban climate network. *Urban Climate*, 44. https://doi.org/10.1016/j.uclim.2022.101207

Bhatnagar, M., Mathur, J., & Garg, V. (2018). Determining base temperature for heating and cooling degree-days for India. *Journal of Building Engineering*, 18, 270–280. https://doi.org/10.1016/j.jobe.2018.03.020

Bueno, B., Norford, L., Hidalgo, J., & Pigeon, G. (2013). The urban weather generator. *Journal of Building Performance Simulation*, 6(4), 269–281. https://doi.org/10.1080/19401493.2012.718797

Bueno, B., Roth, M., Norford, L., & Li, R. (2014). Computationally efficient prediction of canopy level urban air temperature at the neighbourhood scale. *Urban Climate*, 9, 35–53. https://doi.org/10.1016/j.uclim.2014.05.005

Cao, Q., Huang, H., Hong, Y., Huang, X., Wang, S., Wang, L., & Wang, L. (2022). Modeling intra-urban differences in thermal environments and heat stress based on local climate zones in central Wuhan. *Building and Environment*, 225, 109625. https://doi.org/10.1016/j.buildenv.2022.109625

Chen, M., Ban-Weiss, G. A., & Sanders, K. T. (2018). The role of household level electricity data in improving estimates of the impacts of climate on building electricity use. *Energy and Buildings*, 180, 146–158. https://doi.org/10.1016/j.enbuild.2018.09.012

Deng, Z., Javanroodi, K., Nik, V. M., & Chen, Y. (2023). Using urban building energy modeling to quantify the energy performance of residential buildings under climate change. *Building Simulation*, 16(9), 1629–1643. https://doi.org/10.1007/s12273-023-1032-2

Dosio, A., Mentaschi, L., Fischer, E. M., & Wyser, K. (2018). Extreme heat waves under 1.5 °c and 2 °c global warming. *Environmental Research Letters*, 13(5). https://doi.org/10.1088/1748-9326/aab827

Ellena, M., Breil, M., & Soriani, S. (2020). The heat-health nexus in the urban context: A systematic literature review exploring the socio-economic vulnerabilities and built environment characteristics. *Urban Climate*, 34, 100676. https://doi.org/10.1016/j.uclim.2020.100676

Elzeni, M., Elmokadem, A., & Badawy, N. M. (2022). Classification of urban morphology indicators towards urban generation. *Port Said Engineering Research Journal*, 26(1), 43–56. https://doi.org/10.21608/pserj.2021.91760.1135

Heaviside, C., Macintyre, H., & Vardoulakis, S. (2017). The Urban Heat Island: Implications for Health in a Changing Environment. *Current Environmental Health Reports*, 4(3), 296–305. https://doi.org/10.1007/s40572-017-0150-3

Heidelberger, E., & Rakha, T. (2022). Inclusive urban building energy modeling through socioeconomic data: A persona-based case study for an underrepresented community. *Building and Environment*, 222, 109374. https://doi.org/10.1016/J.BUILDENV.2022.109374

Heris, M. P., Middel, A., & Muller, B. (2020). Impacts of form and design policies on urban microclimate: Assessment of zoning and design guideline choices in urban redevelopment projects. *Landscape and Urban Planning*, 202, 103870. https://doi.org/10.1016/j.landurbplan.2020.103870

Hong, T., Chen, Y., Luo, X., Luo, N., & Lee, S. H. (2020). Ten questions on urban building energy modeling. *Building and Environment*, 168, 106508. https://doi.org/10.1016/J.BUILDENV.2019.106508

Hood, R. (2005). Global Warming. *A Companion to Applied Ethics*, 674–684. https://doi.org/10.1002/9780470996621.ch50

Huo, X., Yang, L., Li, D. H. W., Lun, I., Lou, S., & Shi, Y. (2022). Impact of climate change on outdoor design conditions and implications to peak loads. *Building Simulation*, 15(12), 2051–2065. https://doi.org/10.1007/s12273-022-0913-0

Jain, A. K. (2010). Data clustering: 50 years beyond K-means. *Pattern Recognition Letters*, 31(8), 651–666. https://doi.org/10.1016/j.patrec.2009.09.011

Javanroodi, K., Mahdavinejad, M., & Nik, V. M. (2018). Impacts of urban morphology on reducing cooling load and increasing ventilation potential in hot-arid climate. *Applied Energy*, 231, 714–746. https://doi.org/10.1016/j.apenergy.2018.09.116

Joshi, M. Y., Rodler, A., Musy, M., Guernouti, S., Cools, M., & Teller, J. (2022). Identifying urban morphological archetypes for microclimate studies using a clustering approach. *Building and Environment*, 224, 109574. https://doi.org/10.1016/j.buildenv.2022.109574

Karthik, D. (2021, December 25). *Trichy corporation to have five zones*. Times of India . https://timesofindia.indiatimes.com/city/trichy/trichy-corporation-to-have-five-zones/articleshowprint/88486041.cms

Katal, A., Mortezazadeh, M., Wang, L. (Leon), & Yu, H. (2022). Urban building energy and microclimate modeling – From 3D city generation to dynamic simulations. *Energy*, 251, 123817. https://doi.org/10.1016/j.energy.2022.123817

Klysik, K., & Fortuniak, K. (1999). Temporal and spatial characteristics of the urban heat island of Lodz, Poland. *Atmospheric Environment*, 33(24–25), 3885–3895. https://doi.org/10.1016/S1352-2310(99)00131-4

Kotharkar, R., & Bagade, A. (2018). Local Climate Zone classification for Indian cities: A case study of Nagpur. *Urban Climate*, 24, 369–392. https://doi.org/10.1016/j.uclim.2017.03.003

Kotharkar, R., Ghosh, A., Kapoor, S., & Reddy, D. G. K. (2022). Approach to local climate zone based energy consumption assessment in an Indian city. *Energy and Buildings*, 259, 111835. https://doi.org/10.1016/j.enbuild.2022.111835

Leconte, F., Bouyer, J., Claverie, R., & Pétrissans, M. (2015). Estimation of spatial air temperature distribution at sub-mesoclimatic scale using the LCZ scheme and mobile measurements. In *Proceedings of the 9th International Conference on Urban Climate & 12th Symposium on Urban Environment* (pp. 1–12).

Li, X., Zhou, Y., Yu, S., Jia, G., Li, H., & Li, W. (2019). Urban heat island impacts on building energy consumption: A review of approaches and findings. *Energy*, 174, 407–419. https://doi.org/10.1016/j.energy.2019.02.183

Li, Y., Wang, W., Wang, Y., Xin, Y., He, T., & Zhao, G. (2021). A review of studies involving the effects of climate change on the energy consumption for building heating and cooling. *International Journal of Environmental Research and Public Health*, 18(1), 40. https://doi.org/10.3390/ijerph18010040

Ma, L., Yan, Z., He, W., Lv, L., He, G., & Li, M. (2023). Towards better exploiting object-based image analysis paradigm for local climate zones mapping. *ISPRS Journal of Photogrammetry and Remote Sensing*, 199, 73–86. https://doi.org/10.1016/j.isprsjprs.2023.03.018

Masson, V., Lemonsu, A., Hidalgo, J., & Voogt, J. (2020). Urban climates and climate change. *Annual Review of Environment and Resources*, 45, 411–444. https://doi.org/10.1146/annurev-environ-012320-083623

Nagpal, S., Hanson, J., & Reinhart, C. (2019). A framework for using calibrated campus-wide building energy models for continuous planning and greenhouse gas emissions reduction tracking. *Applied Energy*, 241, 82–97. https://doi.org/10.1016/j.apenergy.2019.03.010

Nassar, A. K., Blackburn, G. A., & Whyatt, J. D. (2016). Dynamics and controls of urban heat sink and island phenomena in a desert city: Development of a local climate zone scheme using remotely-sensed inputs. *International Journal of Applied Earth Observation and Geoinformation*, 51, 76–90. https://doi.org/10.1016/j.jag.2016.05.004

Nastran, M., Kobal, M., & Eler, K. (2019). Urban heat islands in relation to green land use in European cities. *Urban Forestry and Urban Greening*, 37, 33–41. https://doi.org/10.1016/j.ufug.2018.01.008

Natanian, J., & Auer, T. (2020). Beyond nearly zero energy urban design: A holistic microclimatic energy and environmental quality evaluation workflow. *Sustainable Cities and Society*, 56, 102094. https://doi.org/10.1016/j.scs.2020.102094

Nik, V. M. (2016). Making energy simulation easier for future climate – Synthesizing typical and extreme weather data sets out of regional climate models (RCMs). *Applied Energy*, 177, 204–226. https://doi.org/10.1016/J.APENERGY.2016.05.107

Oke, T. R. (2004). Initial guidance to obtain representative meteorological observations at urban sites. *World Meteorological Organization*, 81, 51.

Palusci, O., Monti, P., Cecere, C., Montazeri, H., & Blocken, B. (2022). Impact of morphological parameters on urban ventilation in compact cities: The case of the Tuscolano-Don Bosco district in Rome. *Science of the Total Environment*, 807, 150490. https://doi.org/10.1016/j.scitotenv.2021.150490

Panuwatwanich, K., & Nguyen, T. T. (2017). Influence of Total Quality Management on Performance of Vietnamese Construction Firms. *Procedia Engineering*, 182, 548–555. https://doi.org/10.1016/j.proeng.2017.03.151

Parmesan, C. & Yohe, G. (2003). A globally coherent fingerprint of climate change impacts across natural systems. *Nature*, 421, 37–42 (2003). https://doi.org/10.1038/nature01286

Perkins-Kirkpatrick, S. E., & Lewis, S. C. (2020). Increasing trends in regional heatwaves. *Nature Communications*, 11, 3357. https://doi.org/10.1038/s41467-020-16970-7

Rajagopal, P., Priya, R. S., & Senthil, R. (2023). A review of recent developments in the impact of environmental measures on urban heat island. *Sustainable Cities and Society*, 88, 104279. https://doi.org/10.1016/j.scs.2022.104279

Schirmer, P. M., & Axhausen, K. W. (2016). A multiscale classification of urban morphology. *Journal of Transport and Land Use*, 9(1), 101–130. https://doi.org/10.5198/jtlu.2015.667

Skarbit, N., Stewart, I. D., Unger, J., & Gál, T. (2017). Employing an urban meteorological network to monitor air temperature conditions in the 'local climate zones' of Szeged, Hungary. *International Journal of Climatology*, 37, 582–596. https://doi.org/10.1002/joc.5023

Stewart, I. D. (2011). A systematic review and scientific critique of methodology in modern urban heat island literature. *International Journal of Climatology*, 31(2), 200–217. https://doi.org/10.1002/joc.2141

Stewart, I. D., & Oke, T. R. (2012). Local climate zones for urban temperature studies. *Bulletin of the American Meteorological Society*, 93(12), 1879–1900. https://doi.org/10.1175/BAMS-D-11-00019.1

Sun, L., Chen, J., Li, Q., & Huang, D. (2020). Dramatic uneven urbanization of large cities throughout the world in recent decades. *Nature Communications*, 11(1). https://doi.org/10.1038/s41467-020-19158-1

Taha, H. (1997). Urban climates and heat islands: Albedo, evapotranspiration, and anthropogenic heat. *Energy and Buildings*, 25(2), 99–103. https://doi.org/10.1016/s0378-7788(96)00999-1

Teller, J., & Azar, S. (2001). Townscope II - A computer systems to support solar access decision-making. *Solar Energy*, 70(3), 187–200. https://doi.org/10.1016/S0038-092X(00)00097-9

United Nations. (2019). *World population prospects 2019: Volume I, comprehensive tables*. Department of Economic and Social Affairs.

Vallati, A., De Lieto Vollaro, A., Golasi, I., Barchiesi, E., & Caranese, C. (2015). On the impact of urban micro climate on the energy consumption of buildings. *Energy Procedia*, 82, 506–511. https://doi.org/10.1016/j.egypro.2015.11.862

Wang, D., Landolt, J., Mavromatidis, G., Orehounig, K., & Carmeliet, J. (2018). CESAR: A bottom-up building stock modelling tool for Switzerland to address sustainable energy transformation strategies. *Energy*

and Buildings, 169, 9–26. https://doi.org/10.1016/J.ENBUILD.2018.03.020

Warren, E. L., Young, D. T., Chapman, L., Muller, C., Grimmond, C. S. B., & Cai, X. M. (2016). The Birmingham Urban Climate Laboratory-A high density, urban meteorological dataset, from 2012-2014. *Scientific Data*, 3. https://doi.org/10.1038/sdata.2016.38

Yang, Y., Javanroodi, K., & Nik, V. M. (2021). Climate change and energy performance of European residential building stocks – A comprehensive impact assessment using climate big data from the coordinated regional climate downscaling experiment. *Applied Energy*, 298, 117246. https://doi.org/10.1016/J.APENERGY.2021.117246

Yang, R., Yang, J., Wang, L., Xiao, X., & Xia, J. (2022). Contribution of local climate zones to the thermal environment and energy demand. *Frontiers in Public Health*, 10. https://doi.org/10.3389/fpubh.2022.992050

Yue, W., Liu, X., Zhou, Y., & Liu, Y. (2019). Impacts of urban configuration on urban heat island: An empirical study in China mega-cities. *Science of the Total Environment*, 671, 1036–1046. https://doi.org/10.1016/j.scitotenv.2019.03.421